INVESTIGATION ON EFFECTIVE APPROACHES OF BRAIN FE MODELING TO IMPROVE ITS VALIDATION PERFORMANCE ON BRAIN DEFORMATION DURING HEAD IMPACT

Noritoshi Atsumi
Yuko Nakahira
Masami Iwamoto
Toyota Central R&D Labs., Inc.
Japan

Paper Number 23-0094

ABSTRACT

The finite element (FE) model of the human brain is an effective tool for predicting brain strain during head impacts that can result in traumatic brain injury (TBI). Although many brain FE models have been proposed and updated upon thus far, it was unclear what kind of modeling approaches would critically contribute to improving the biofidelity of the models. This study investigated whether the implementation of material anisotropy of the brain tissue or the appropriate representation of the boundary conditions around the ventricle would affect the validation performance of modeling brain deformation during head impact. Axonal fiber tracts of the whole brain were extracted from diffusion-weighted images in the Amsterdam Open MRI Collection using tractography. The direction of the material axis in each element of the white matter of the previously developed human brain FE model was determined based on axonal fiber tracts. Incompressible fluid dynamics (ICFD), including perfusion pressure, was also applied to the intraventricular cerebrospinal fluid (CSF) of the model. Validation of the displacement and strain in the brain during head impact was performed based on cadaveric test data, wherein quantitative evaluation of validation accuracy was conducted using the CORrelation and Analysis (CORA) method. The CORA scores of the model were compared with those of the model with isotropic material or those of the model without ICFD. The difference in CORA scores for brain displacement was minimal among the models. On the other hand, the CORA scores for brain strain of the model with ICFD were higher than those without ICFD. However, CORA scores for the brain strain of the anisotropic model based on the axonal fiber tracts were similar to or lower than those of the isotopic model. Comparing CORA scores among the models indicated that introducing ICFD to the intraventricular CSF improved the validation performance of the brain FE model. However, implementing anisotropy of the white matter based on tractography at the element level does not necessarily improve the validation performance of the brain FE model. In addition, evaluating the validation accuracy of the brain FE model using brain displacement did not reflect the difference in the accuracy of predicting brain strain during head impact. A limitation of this study includes the spatial registration of axonal fiber tracts with the FE model using affine transformation. It would be more desirable to consistently conduct FE modeling and tract extraction so that the differences in brain geometry and axonal fiber pathways for each subject could be considered. The findings in this study indicate that the appropriate representation of the boundary condition around the ventricle using ICFD would affect the validation performance on the brain strain in the brain FE model rather than the accuracy of the description of the anisotropy at the element level. These findings may provide useful insights into modeling strategies of the human brain to predict TBI due to head impact associated with traffic accidents.

INTRODUCTION

Mild traumatic brain injury (mTBI) or concussions account for approximately 80% of traumatic brain injury (TBI) incidents, which can result from a numerous causes, including blunt trauma caused by falls, vehicular accidents, and collisions experienced in sports-related activities associated with angular acceleration of the head [1, 2]. As mTBI requires careful treatment and incurs large healthcare costs [3, 4], predicting and preventing the occurrence of mTBI in such situations is important.

The finite element (FE) model of the human brain is an effective tool for predicting deformations of brain tissues or axons during head impact. Many human brain FE models have been developed and continually updated in recent years [5–11]. Several strategies for improving the biofidelity of the human brain FE model comprise refining the representation of the anatomical structure, including the gyrus or limbic system; application of the constitutive model describing the anisotropy and viscoelasticity of the brain tissue; explicit implementation of the axonal fiber tracts; and consideration of the dynamics of the intracranial cerebrospinal fluid (CSF). However, it was unclear what kind

of modeling approaches would critically contribute to improving the biofidelity of the brain FE model. In addition, despite the suggested possibility of using brain or axonal strain to predict mTBI [5, 12–14], only a few models provide their validation performance with respect to the brain strain during head impact [8, 9, 11].

In this study, the axonal fiber orientation extracted from tractography was applied in the direction of the material axis in a previously developed human brain FE model [15]. By comparing the validation scores to those of the brain FE model and considering intraventricular fluid dynamics using incompressible fluid dynamics (ICFD) [11], we investigated whether the implementation of material anisotropy of brain tissue or the appropriate representation of the boundary conditions around the ventricle may affect the validation accuracy of the brain deformation.

MATERIALS AND METHODS

Extraction of Axonal Fiber Tracts

Diffusion-weighted images (DWI) and T1-weighted images (T1WI) required for the extraction of axonal fiber tracts were obtained from the pre-processed Amsterdam Open MRI Collection (AOMIC) dataset [16]. The spatial resolution of DWI is 2.0×2.0×2.0 mm^3, whereas that of T1WI is 1.0×1.0×1.0 mm^3. The b-values of DWI, which represent the diffusion intensity, were 0 and 1,000 s/mm^2. These two values are required to separate the white matter tissue from the rest of the brain compartment in DWI using the difference in the response functions of fiber orientation distribution. Based on the published tutorials of tractography [17], MRtrix v3.0.0 [18, 19] and dependent software, including FSL (FMRIB Software Lilbrary) [20], FreeSurfer [21], and Advanced Normalization Tools (ANTs) [22] were utilized to extract two million axonal fiber tracts across the whole brain. After extracting the tracts of the whole brain, structural connectivity was derived for each subject based on the number of axonal fiber tracts. Structural connectivity refers to the degree of connection between any two regions, when the cortical and subcortical parts of the whole brain are divided into several functional and anatomical regions. Ideally, the average tract data across the subjects should be introduced into the brain FE model. However, as the geometry of the brain differs among subjects and the extracted axonal fiber tracts are specific to each subject, deriving average tracts were not possible. Therefore, in this study, the subject with the smallest variance in structural connectivity was selected from all the subjects (n = 216) in the AOMIC dataset. Figure 1 shows the axonal fiber tracts extracted from the DWI data of the selected subject, in which the T1WI was overlayed; only a representative 20,000 tracts out of two million tracts are shown.

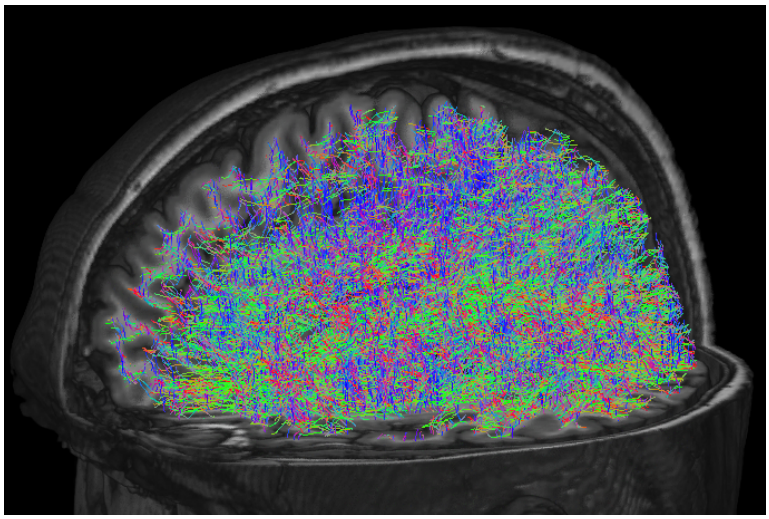

Figure 1. Axonal fiber tracts (color) extracted from DWI with overlayed T1WI (grayscale). Only a representative 20,000 tracts are shown here.

Human Brain FE Model

A previously developed human brain FE model [11, 15] was used in this study. The left side of Figure 2 shows an overview of the model. The model has a well-described anatomical structure, including the cerebrum, corpus callosum, thalamus, basal ganglia, fornix, cerebellum, dura mater, falx, tentorium, midbrain, pons, and medulla oblongata using hexahedral solid elements. The pia mater and arachnoid were modeled using shell elements. The model contained 48,313 solid elements and 13,032 shell elements. The interface between the brain and dura mater was modeled using a layer of solid elements with shared nodes.

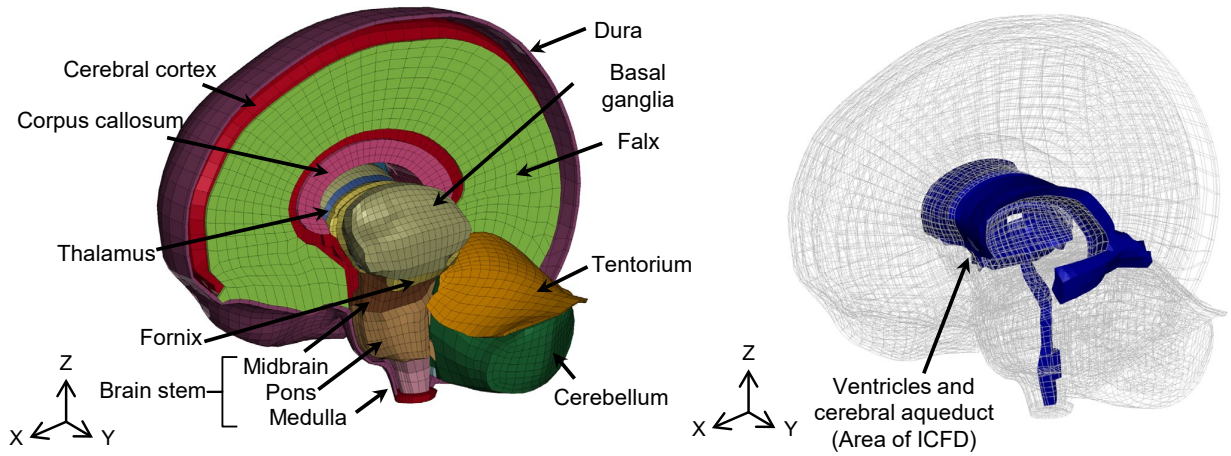

Figure 2. (left) Human brain FE model used in this study. (right) The area in which ICFD was applied.

The material properties in each part of the brain FE model followed those of the previous model [11]. A constitutive model utilized in the brain parenchyma appropriately describes the anisotropy in white matter, strain-rate dependency, and characteristic features of the unloading process [15, 23]. In this study, the material axes in each solid were determined based on the orientation of the extracted axonal fiber tracts. First, the coordinates of each fiber tract were obtained at 1 mm intervals using *tckresample* and *tckconvert* commands in MRtrix. Then, spatial registration of the coordinates of the tracts toward FE model was performed using affine transformation. As the DWI obtained from the AOMIC dataset covered the brainstem and cerebellum incompletely, the tracts in these regions were interrupted in the middle. Therefore, affine transformation was applied to align the outermost points of the top, bottom, left, right, front, and rear, based on the coordinates of tracts belonging to the cerebral part. An overview of axonal fiber tracts registered with the brain FE model is shown in the left part of Figure 3. Next, each vector of the registered tracts was checked if it had passed through each solid element of the cerebral part of the FE model. The average value of the vectors to be passed then was set as the material axis of the solid element. The right side of Figure 3 shows a conceptual diagram of the procedure. It is not possible to distinguish the starting or ending side from the extracted axonal fiber tracts. Therefore, even if the axial directions of the tracts are similar, they may cancel each other when averaged, depending on the direction of the vectors. To address this, the directions of each vector were unified based on the following equations:

$$\boldsymbol{v} = \begin{cases} \boldsymbol{v} & (\mathrm{prod}(\boldsymbol{v}) \geq 0) \\ -\boldsymbol{v} & (\mathrm{prod}(\boldsymbol{v}) < 0) \end{cases} \qquad \text{Equation (1)}$$

The symbol $\boldsymbol{v}$ is a three-dimensional vector corresponding to the direction of the tracts. Function prod$(\cdot)$ derives the product of the vector components. The material axes for each element are defined using the keyword *ELEMENT_SOLID_ORTHO in LS-DYNA (LSTC, USA).

To introduce fluid dynamics into the intraventricular CSF, the ICFD option of LS-DYNA was used, as in a previous study [11]. ICFD was applied to the lateral ventricle, third ventricle, fourth ventricle, and cerebral aqueduct of the brain FE model, indicated in blue in the right part of Figure 2. When a closed space is provided by surface shell elements defined as the boundary, the ICFD solver in LS-DYNA automatically generates a fluid volume mesh inside

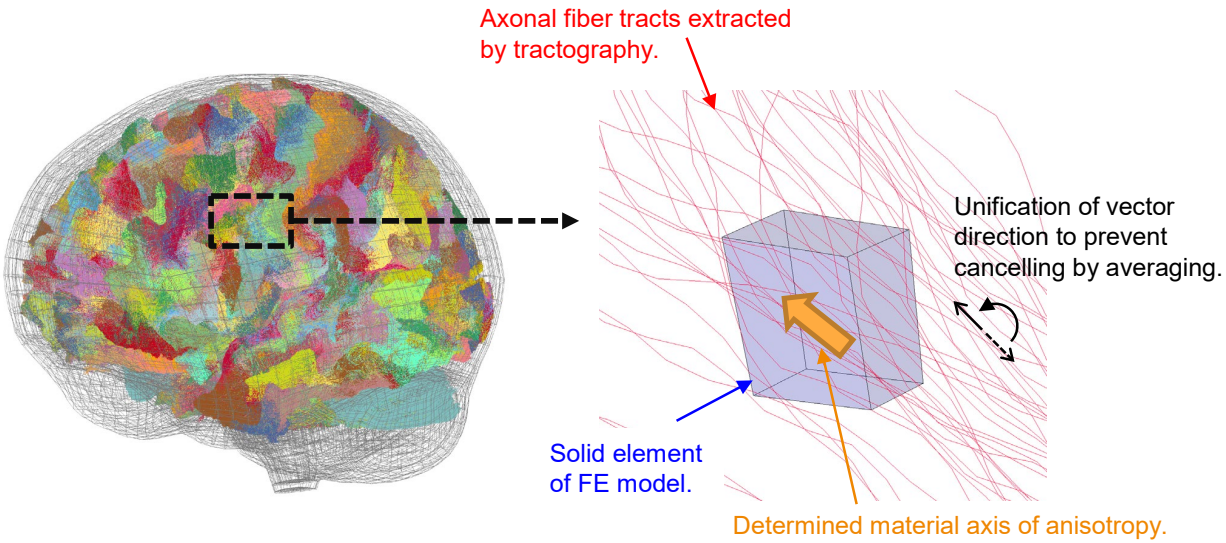

Figure 3. (left) Axonal fiber tracts registered with the brain FE model. (right) Determination of the material axis of each solid element.

the space at the start of the analysis. The boundary condition between the fluid and structure was a non-slip condition, and three boundary layer meshes were defined. In addition, intracranial perfusion pressure was considered. Based on the experimental setting in the PMHS test performed by Hardy et al. [24], an initial pressure of 10.3 kPa was applied to the area of ICFD. The fluid-structural interaction was solved in a weak coupling, that is, the solid and fluid solvers separately proceeded with the calculations using individual time steps, and the interpolated displacements and forces at the boundary between the structure and fluid were passed to each other [25]. The time step for solving the ICFD was 1.0e-5 s, whereas that for the structure was 8.96e-8 s in this study. All FE analyses were conducted using the LS-DYNA R11.1.0 SMP with double precision.

Validation Setting

The validation protocol of the FE model followed that of a previous study [11]. PMHS test data on brain deformation during head impacts, which were originally obtained by Hardy et al. [24] and subsequently reanalyzed with respect to the strain calculation by Zhou et al. [26, 27], were used. Three representative tests were performed. C288-T3 was an occipital impact test resulting in forward rotation of the head with a peak angular acceleration of 24.2 krad/s^2 (Figure 4(a)). C380-T1 was a parietal impact test resulting in right lateral flexion with a peak angular acceleration of 5.1 krad/s^2 (Figure 4(b)). C380-T2 was an occipital impact test resulting in the left rotation of the head with a peak angular acceleration of 5.1 krad/s^2 (Figure 4(c)). In these experiments, the displacements of each of the seven neural density targets (NDT) in the two clusters (C1 and C2) embedded in the head of the PMHS with respect to its center of gravity (CG) were measured using a high-speed biplanar X-ray system during head impact [24]. The cluster strain was calculated from the relative displacements of the NDTs in each cluster. To simulate the experiments, a cluster model comprising eight tetrahedral elements was prepared (Figure 4(d)) First, simulations for each case using the brain FE model were performed to calculate the displacements of the nodes closest to each NDT. Subsequently, the history of the displacements of the nodes was input to the corresponding NDT in the cluster model. Finally, the cluster strain was calculated by averaging the Green–Lagrange strain of each element in the cluster model. The four tetrahedral elements in C2 were not included in the cluster strain calculations for C380-T1 and C380-T2 because of lack of data for the 9th NDT of C2.

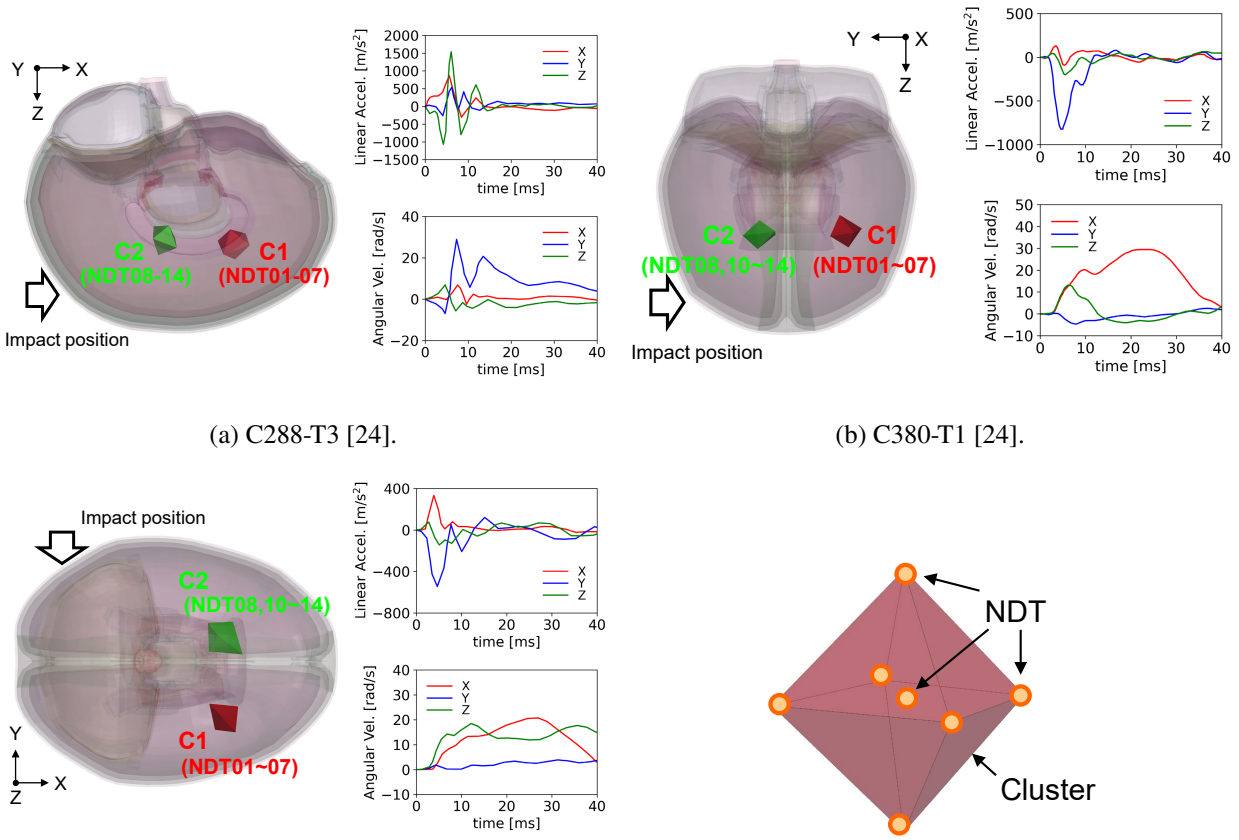

(a) C288-T3 [24].

(b) C380-T1 [24].

(c) C380-T2 [24].

(d) Cluster model composed of eight tetrahedron elements.

Figure 4. Validation setting.

To compare the influence of different modeling approaches on the validation results, four different models shown in Table 1 were prepared. In Models A and B, the constitutive model with isotropic parameters, which was identified against gray matter, was also applied to white matter. On the other hand, the anisotropic constitutive model was utilized for the white matter in Models C and D following the introduction of the axonal fiber tracts as the direction of material axis described above. The intraventricular CSF in Models A and C was modeled using viscoelastic solid elements according to Mao et al. [6], whereas those in Models B and D were described using ICFD with perfusion pressure based on a previous study [11].

Table 1.
List of models compared in this study.

	Material property of brain parenchyma	**Modeling approach of intraventricular CSF**
Model A	isotropic	viscoelastic solid elements [6]
Model B	isotropic	ICFD with perfusion pressure [11]
Model C	anisotropic based on tracts	viscoelastic solid elements [6]
Model D	anisotropic based on tracts	ICFD with perfusion pressure [11]

The validation results of the displacements of NDTs and the strain of each cluster were quantitatively evaluated based on the CORrelation and Analysis (CORA) method [28, 29]. The CORA method assesses the degree of correlation between a pair of time-history curves using two sub-methods: the corridor method and the correlation method. However, the corridor method was not activated, and the recommended setting was used in this study, referring to the work of Giordano and Kleiven [30]. The CORA score ranges from 0 to 1, with closer to 1 indicating a better match.

The sliding scales of CORA are defined as follows: “Unacceptable”:0.0-0.26, “Marginal”:0.26-0.44, “Fair”:0.44-0.65, “Good”:0.65-0.86, “Excellent”:0.86-1.0 [31].

RESULTS

As a typical result, comparisons of the histories of the displacements in NDTs belonging to each cluster for C380-T1 between the experimental data [24] and the simulation results using the brain FE models were shown in Figures 5 and 6, respectively (for C288-T3 and C380-T2, see Figures A1-A4 in Appendix). The displacements in the direction of the X-axis in NDT01, 05, 06, Y-axis in NDT01, 04-06, 12, and Z-axis in NDT06, 08-14 of Models B and D were larger than those of Models A and C. However, no noticeable difference in the overall trends of the displacement of NDTs was observed among the models.

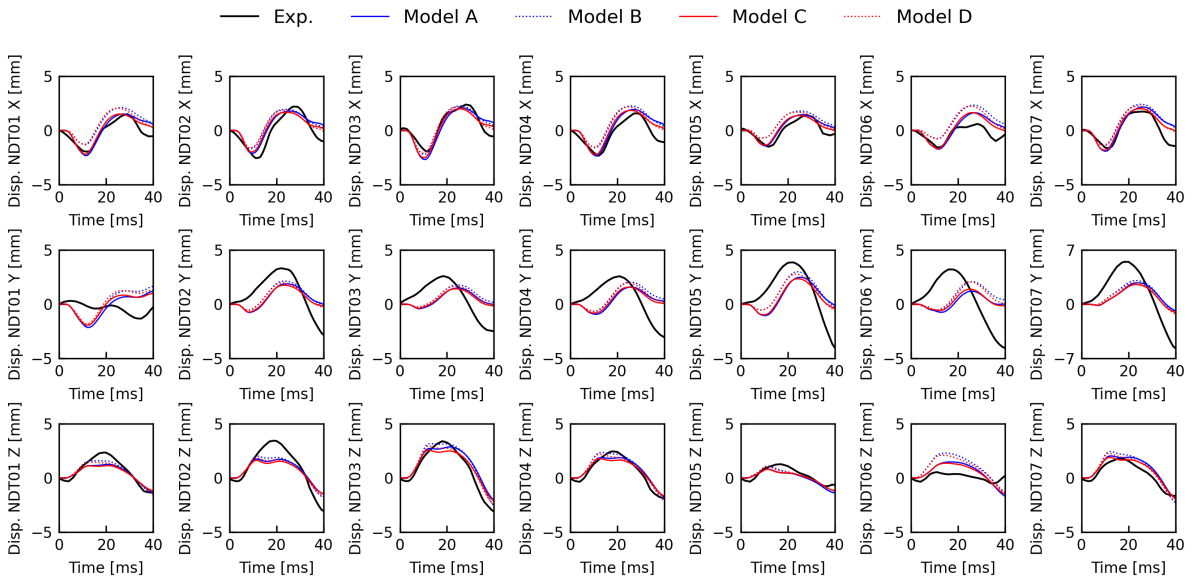

Figure 5. Comparisons of the histories of displacements in NDTs belonging to C1 for C380-T1 between the PMHS test data [24] and the simulation results.

Figure 7 shows the comparisons of the histories of the maximum principal strain (MPS) and maximum shear strain (MSS) in both clusters for C380-T2 between the reanalyzed data [27] and simulation results using the brain FE models (for C288-T3 and C380-T1, see Figures A5 and A6 in the Appendix). The peak strain values in C1 were higher for Models B, A, D, and C, in this order. In contrast, for C2, the order was Models B, D, A, and C. In addition, Models A and C and Models B and D had similar waveforms in both clusters.

Tables 2 and 3 show comparisons of the CORA scores on the displacement of NDTs and strain in clusters for each test, respectively. The values indicated in Table 2 are the average scores of displacements in the 14 NDTs of both clusters, whereas those in Table 3 are the average scores of MPS and MSS in both clusters. For comparison, the CORA scores reported by Li et al. [8], who proposed a detailed and personalizable (ADAPT) head model, are also provided in these tables. From Table 2, the scores on the displacements in NDTs for C380-T1 and C380-T2 were almost equivalent among the four brain FE models. The scores on the displacements in NDTs for C288-T3 using Models B and D were slightly higher than those using Models A and C. However, the difference in scores was insufficient to cross the sliding scale of CORA. The CORA scores for the NDT displacements in this study were comparable to those in the ADAPT head model [8].

Conversely, the CORA scores on the strain of the clusters varied considerably among the models, as shown in Table 3. Model C resulted in the lowest CORA scores in all the tests. For C380-T1 and C380-T2, the CORA scores for the cluster strain in Models A, B, and D were almost equivalent. In contrast, the scores for C288-T3 using Models B and D were higher than those using Models A and C. The highest average score of CORA in the three tests was found in

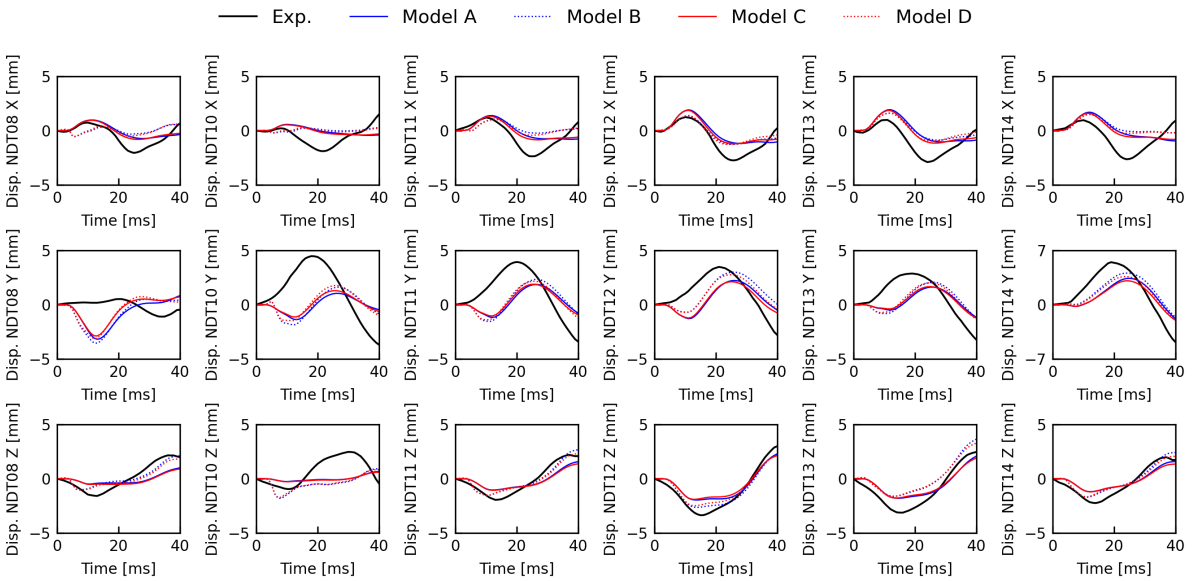

Figure 6. Comparisons of the histories of displacements in NDTs belonging to C2 for C380-T1 between the PMHS test data [24] and the simulation results.

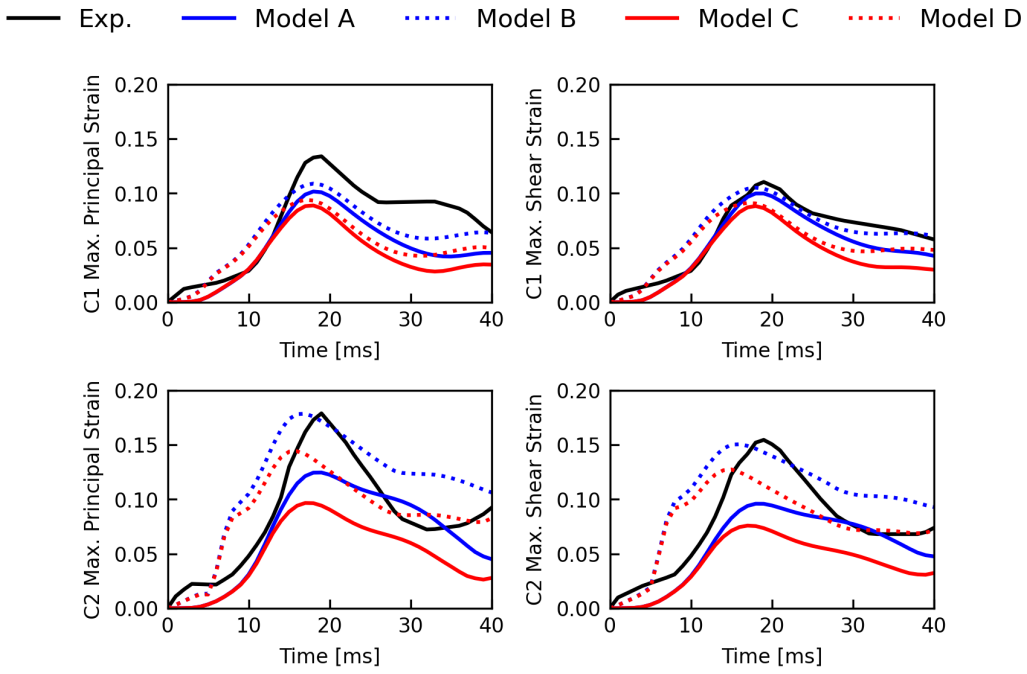

Figure 7. Comparisons of the histories of strain in C1 and C2 for C380-T2 between the PMHS test data [24, 27] and the simulation results.

Model D. In C288-T3 and C380-T2, the CORA scores for the cluster strain in Models B and D were higher than those in the ADAPT head model [8].

Table 2.
Comparisons of averaged CORA score on the displacement of all NDTs.

	Model A	**Model B**	**Model C**	**Model D**	**ADAPT** [8]
C288-T3	0.574 (Fair)	0.634 (Fair)	0.565 (Fair)	0.620 (Fair)	0.588 (Fair)
C380-T1	0.676 (Good)	0.688 (Good)	0.688 (Good)	0.694 (Good)	0.694 (Good)
C380-T2	0.558 (Fair)	0.571 (Fair)	0.538 (Fair)	0.550 (Fair)	0.549 (Fair)
Ave.	0.603	0.631	0.597	0.621	0.610

Table 3.
Comparisons of averaged CORA score on the strain of both clusters.

	Model A	**Model B**	**Model C**	**Model D**	**ADAPT** [8]
C288-T3	0.648 (Fair)	0.904 (Excellent)	0.626 (Fair)	0.890 (Excellent)	0.742* (Good)
C380-T1	0.820 (Good)	0.809 (Good)	0.751 (Good)	0.836 (Good)	0.877* (Excellent)
C380-T2	0.866 (Excellent)	0.900 (Excellent)	0.779 (Good)	0.904 (Excellent)	0.793* (Good)
Ave.	0.778	0.871	0.719	0.877	0.804

* Averaged scores of MPS and MSS only from C1 for ADAPT model.

DISCUSSION

This study provides quantitative comparisons of validation performance on the displacement and strain in the brain among the brain FE models based on different modeling approaches with respect to the anisotropy of the brain tissue and boundary conditions around the ventricle. As shown in Table 2, the CORA scores for NDT displacement were almost equivalent among the models. In other words, both the implementation of the material axis in the brain tissue based on the axonal fiber tracts and the application of ICFD to the intraventricular CSF had minimal effect on the validation performance of the displacement in the brain. However, as shown in Table 3, the application of ICFD resulted in improved CORA scores on cluster strain. This trend is consistent with that reported in a previous study [11]. However, implementing the material axis based on axonal fiber tracts with the present method does not necessarily improve the CORA scores on cluster strain. These findings suggest that the appropriate representation of the boundary condition around the ventricle using ICFD affects the validation performance of strain in the brain more than the accuracy of the description of anisotropy at the element level. In addition, evaluating the validation performance of the brain FE model using NDT displacements could not reflect the difference in the accuracy of predicting brain strain during head impact. This is consistent with findings in previous studies that validation solely based on relative brain–skull displacements does not infer biofidelity of strain in the model [9] and that validation against brain strain data is recommended [8, 9].

To describe the material axis of anisotropy in the white matter, previous studies have provided methods that apply fractional anisotropy (FA) values extracted from diffusion tensor images (DTI) to the brain FE model [7, 14, 32, 33]. These methods can implement the distribution of the degree of anisotropy in the whole brain because the constitutive models in their studies include parameters associated with the FA value. However, the validation of these models was performed only against the displacement of the brain tissue, and it was unclear whether the implementation of anisotropy actually contributed to improving the validation performance on brain strain. As the constitutive model of the brain parenchyma used in this study did not include the parameter associated with the FA value, the current study only determined the directions of the material axis in each element of the white matter based on the axonal fiber tracts extracted using tractography. Nevertheless, even if we introduce a parameter that describes the distribution of the degree of anisotropy into the current constitutive model, the material properties in regions where the number of axonal fibers is relatively small would only approach isotropic. Considering the current result that the difference in CORA values due to the implementation of ICFD is larger than that due to anisotropy, it can be inferred that the effect of introducing DTI-based FA distribution on the improvement in validation performance of the brain strain will be smaller than the contribution of the boundary condition.

A possible reason why the introduction of anisotropy based on tractography did not improve the validation performance of the brain strain is that the reduction to the element level does not represent the mechanical properties of axonal fibers continuously leading across the brain parenchyma. Recently, Zhou et al. [34] stated that downsampling process in the introduction of the axonal fiber direction extracted from DTI into the FE models could cause some loss of fiber orientation information in each voxel, which compromised the accuracy of tract-related strain, particularly for the model including resolution mismatch between the mesh and voxel. Although their approach did not include the mechanical influence of axons on the deformation of solid elements because the axons were modeled using null material [34], their suggestion would be consistent with the findings of the current study. In other words, the reduction of the extracted tracts to the element level could result in a reduction in the effect of the directional distribution of individual axons on the local deformation of the brain parenchyma.

Another way to introduce axonal fiber tracts into the brain FE model is to implement the tracts explicitly as one-dimensional beam elements embedded in the solid elements proposed by Garimella et al. [35] and Wu et al. [36]. This approach has the potential to achieve a more detailed prediction of mTBI by computing the strain on the axonal fiber itself and associating it with functional impairments in the brain. However, in this approach, the beam and solid elements in the cerebral part of the model represent neurons and surrounding glial cells, respectively. Thus, determining the material parameters and assigning the mass distribution in each part are key issues in properly predicting the local deformation in the brain.

A limitation of this study is related to the procedure of registration of the extracted axonal fiber tracts into the brain FE model. As in a previous study [7], the registration between them was simply performed using an affine transformation. Thus, the FE model and extracted fiber tracts were each based on data from different subjects. Li et al. [8] proposed a morphing approach using a hierarchical image registration pipeline to develop a subject-specific brain FE model that consistently accounts for the geometry and corresponding axonal fiber tracts in the individual brain. Such a modeling approach would be effective for better evaluation of individual mTBIs. Another limitation is the modeling approach for the interface between the brain and dura mater so-called pia-arachnoid complex (PAC) layer, which consists of the arachnoid trabequlae and CSF. In this study, the PAC layer was modeled by not applying ICFD but using viscoelastic solid elements with shared nodes, following previous research [11]. Further experimental or numerical studies are needed to investigate the influence of CSF behavior and perfusion pressure in the PAC layer on brain deformation, thus validating the performance of the brain FE models.

CONCLUSIONS

In this study, we examined the effectiveness of the implementation of the material axis based on the axonal fiber tracts and fluid dynamics of CSF using ICFD on the validation performance of brain deformation in the brain FE model. The results suggested that the appropriate representation of boundary conditions around the ventricle, including ICFD, would affect the validation performance of strain in the brain more than the accuracy of the description of anisotropy at the element level. In addition, evaluating the validation performance of the brain FE model using NDT displacements does not necessarily guarantee the validation accuracy to predict brain strain during head impact. The findings of this study would provide useful insights into modeling strategies of the brain FE model for better prediction of mTBI.

ACKNOWLEDGMENTS

We thank Dr. Hiroyuki Sakai for valuable advice in introducing tractography. We also thank Editage (www.editage.jp) for English language editing.

REFERENCES

[1] Smith, D.H., Nonaka, M., Miller, R., Leoni, M., Chen, X.H., Alsop, D., & Meaney, D.F. 2000. “Immediate coma following inertial brain injury dependent on axonal damage in the brainstem”. J. Neurosurg., Vol. 93, pp. 315–322.

[2] Narayana, P.A. 2017. “White matter changes in patients with mild traumatic brain injury: MRI perspective”. Concussion, Vol. 2, pp. CNC35.

[3] Miller, G.F., DePadilla, L., & Xu, L. 2021. “Costs of nonfatal traumatic brain injury in the United States, 2016”. Med. Care, Vol. 59, pp. 451–455.

[4] Shinoda, J. & Asano, Y. 2013. "Neuroimaging of patients with impairments of executive brain function due to traumatic brain injury". Japanese J. Neurosurg., Vol. 22, pp. 842–848.

[5] Kleiven, S. 2007. "Predictors for traumatic brain injuries evaluated through accident reconstructions.". Stapp Car Crash J., Vol. 51, pp. 81–114.

[6] Mao, H., Zhang, L., Jiang, B., Genthikatti, V.V., Jin, X., Zhu, F., Makwana, R., Gill, A., Jandir, G., Singh, A., & Yang, K.H. 2013. "Development of a Finite Element Human Head Model Partially Validated With Thirty Five Experimental Cases". J. Biomech. Eng., Vol. 135, pp. 111002.

[7] Sahoo, D., Deck, C., & Willinger, R. 2014. "Development and validation of an advanced anisotropic visco-hyperelastic human brain FE model". J. Mech. Behav. Biomed. Mater., Vol. 33, pp. 24–42.

[8] Li, X., Zhou, Z., & Kleiven, S. 2021. "An anatomically detailed and personalizable head injury model: Significance of brain and white matter tract morphological variability on strain". Biomech. Model. Mechanobiol., Vol. 20, pp. 403–431.

[9] Zhao, W. & Ji, S. 2020. "Displacement- and Strain-Based Discrimination of Head Injury Models across a Wide Range of Blunt Conditions". Ann. Biomed. Eng., Vol. 48, pp. 1661–1677.

[10] Zhou, Z., Li, X., & Kleiven, S. 2020. "Biomechanics of Periventricular Injury". J. Neurotrauma, Vol. 37, pp. 1074–1090.

[11] Atsumi, N., Nakahira, Y., & Iwamoto, M. 2021. "Human brain FE modeling including incompressible fluid dynamics of intraventricular cerebrospinal fluid". Brain Multiphysics, Vol. 2, pp. 100037.

[12] Viano, D.C., Casson, I.R., Pellman, E.J., Zhang, L., King, A.I., & Yang, K.H. 2005. "Concussion in professional football: brain responses by finite element analysis: part 9". Neurosurg., Vol. 57, pp. 891–916.

[13] Sahoo, D., Deck, C., & Willinger, R. 2015. "Axonal strain as brain injury predictor based on real-world head trauma simulations", Proceedings of the IRCOBI conference. , No. IRC-15-30, pp. 186–197.

[14] Giordano, C. & Kleiven, S. 2014. "Evaluation of Axonal Strain as a Predictor for Mild Traumatic Brain Injuries Using Finite Element Modeling". Stapp Car Crash J., Vol. 58, pp. 29–61.

[15] Atsumi, N., Nakahira, Y., Tanaka, E., & Iwamoto, M. 2018. "Human brain modeling with its anatomical structure and realistic material properties for brain injury prediction". Ann. Biomed. Eng., Vol. 46, pp. 736–748.

[16] Snoek, L., van der Miesen, M.M., Beemsterboer, T., van der Leij, A., Eigenhuis, A., & Steven Scholte, H. 2021. "The Amsterdam Open MRI Collection, a set of multimodal MRI datasets for individual difference analyses". Scientific Data, Vol. 8, pp. 1–23.

[17] "B.A.T.M.A.N.: Basic and Advanced Tractography with MRtrix for All Neurophiles". https://osf.io/fkyht/.

[18] "MRtrix3". https://www.mrtrix.org/.

[19] Tournier, J.D., Smith, R., Raffelt, D., Tabbara, R., Dhollander, T., Pietsch, M., Christiaens, D., Jeurissen, B., Yeh, C.H., & Connelly, A. 2019. "MRtrix3: A fast, flexible and open software framework for medical image processing and visualisation". NeuroImage, Vol. 202, pp. 116137.

[20] "FSL (FMRIB Software Library)". https://fsl.fmrib.ox.ac.uk/fsl/fslwiki.

[21] "FreeSurfer". https://surfer.nmr.mgh.harvard.edu/.

[22] "ANTs (Advanced Normalization Tools)". http://stnava.github.io/ANTs/.

[23] Atsumi, N., Nakahira, Y., Iwamoto, M., Hirabayashi, S., & Tanaka, E. 2016. "Constitutive Modeling of Brain Parenchyma Taking Account of Strain Rate Dependency with Anisotropy and Application to Brain Injury Analyses", SAE Tech. Pap. , No. 2016-01-1485.

[24] Hardy, W.N., Mason, M.J., Foster, C.D., Shah, C.S., Kopacz, J.M., Yang, K.H., King, A.I., Bishop, J., Bey, M., Anderst, W., & Tashman, S. 2007. "A study of the response of the human cadaver head to impact.". Stapp Car Crash J., Vol. 51, pp. 17–80.

[25] Livermore Software Technology Corporation (LSTC). 2014. “ICFD theory manual: Incompressible fluid solver in LS-DYNA”.

[26] Zhou, Z., Li, X., Kleiven, S., Shah, C.S., & Hardy, W.N. 2018. “A Reanalysis of Experimental Brain Strain Data: Implication for Finite Element Head Model Validation”. Stapp Car Crash J., Vol. 62, pp. 293–318.

[27] Zhou, Z., Li, X., Kleiven, S., & Hardy, W.N. 2019. “Brain Strain from Motion of Sparse Markers”. Stapp Car Crash J., Vol. 63, pp. 1–27.

[28] Gehre, C., Gades, H., & Wernicke, P. 2009. “Objective rating of signals using test and simulation responses”, Proceedings of the 21th ESV Conference. , No. 09-0407.

[29] Gehre, C. & Stahlschmidt, S. 2011. “Assessment of dummy models by using objective rating methods”, Proceedings of the 22nd ESV Conference. , No. 11-0216.

[30] Giordano, C. & Kleiven, S. 2016. “Development of an Unbiased Validation Protocol to Assess the Biofidelity of Finite Element Head Models used in Prediction of Traumatic Brain Injury”. Stapp Car Crash J., Vol. 60, pp. 363–471.

[31] The International Organization for Standardization (ISO). 1999. “Road vehicles — Anthropomorphic side impact dummy — Lateral impact response requirements to assess the biofidelity of the dummy”, ISO/TR 9790:1999.

[32] Wright, R.M. & Ramesh, K.T. 2012. “An axonal strain injury criterion for traumatic brain injury”. Biomechanics and Modeling in Mechanobiology, Vol. 11, pp. 245–260.

[33] Ganpule, S., Daphalapurkar, N.P., Ramesh, K.T., Knutsen, A.K., Pham, D.L., Bayly, P.V., & Prince, J.L. 2017. “A Three-Dimensional Computational Human Head Model That Captures Live Human Brain Dynamics”. Journal of Neurotrauma, Vol. 34, pp. 2154–2166.

[34] Zhou, Z., Wang, T., Jörgens, D., & Li, X. 2022. “Fiber orientation downsampling compromises the computation of white matter tract-related deformation”. J. Mech. Behav. Biomed. Mater., Vol. 132, pp. 105294.

[35] Garimella, H.T., Menghani, R.R., Gerber, J.I., Sridhar, S., & Kraft, R.H. 2019. “Embedded Finite Elements for Modeling Axonal Injury”. Ann. Biomed. Eng., Vol. 47, pp. 1889–1907.

[36] Wu, T., Alshareef, A., Giudice, J.S., & Panzer, M.B. 2019. “Explicit Modeling of White Matter Axonal Fiber Tracts in a Finite Element Brain Model”. Ann. Biomed. Eng., Vol. 47, pp. 1908–1922.

APPENDIX

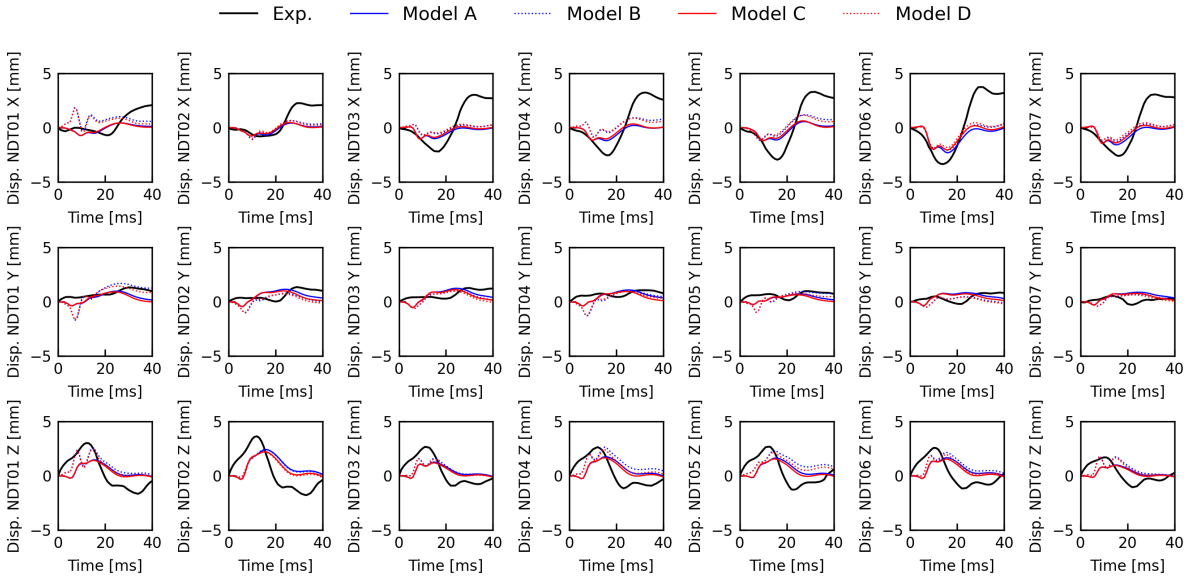

Figure A1. Comparisons of the histories of displacements in NDTs belonging to C1 for C288-T3 between the PMHS test data [24] and the simulation results.

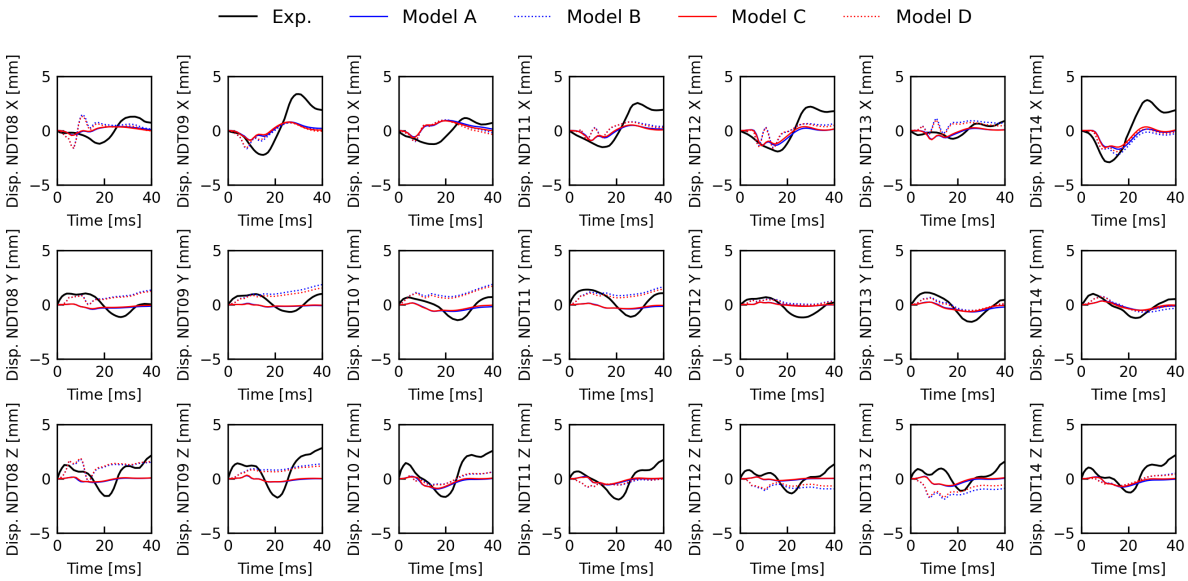

Figure A2. Comparisons of the histories of displacements in NDTs belonging to C2 for C288-T3 between the PMHS test data [24] and the simulation results.

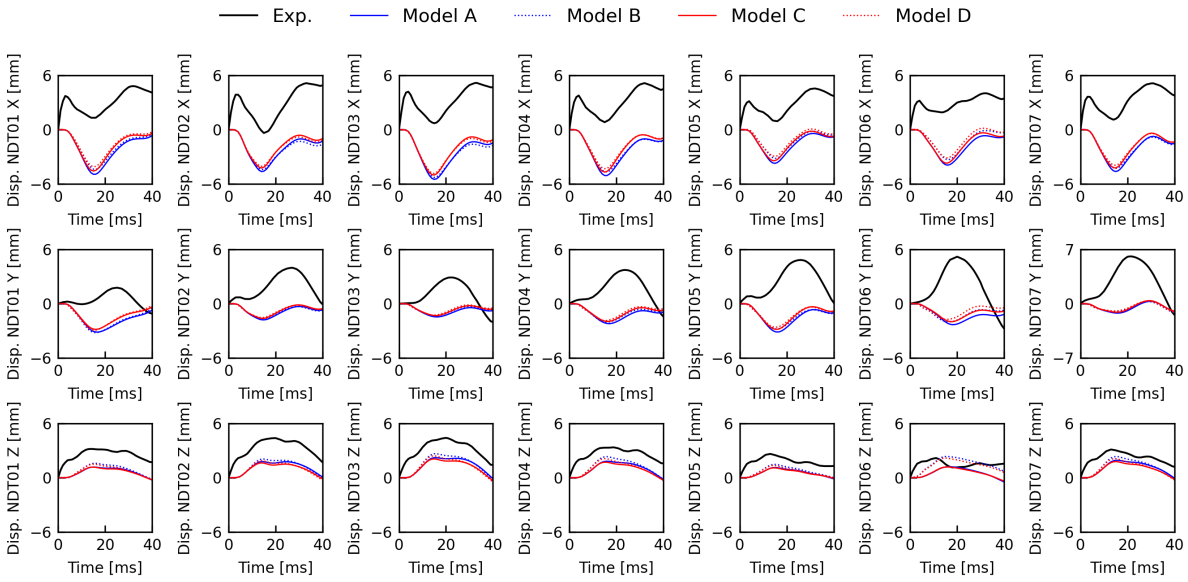

Figure A3. Comparisons of the histories of displacements in NDTs belonging to C1 for C380-T2 between the PMHS test data [24] and the simulation results.

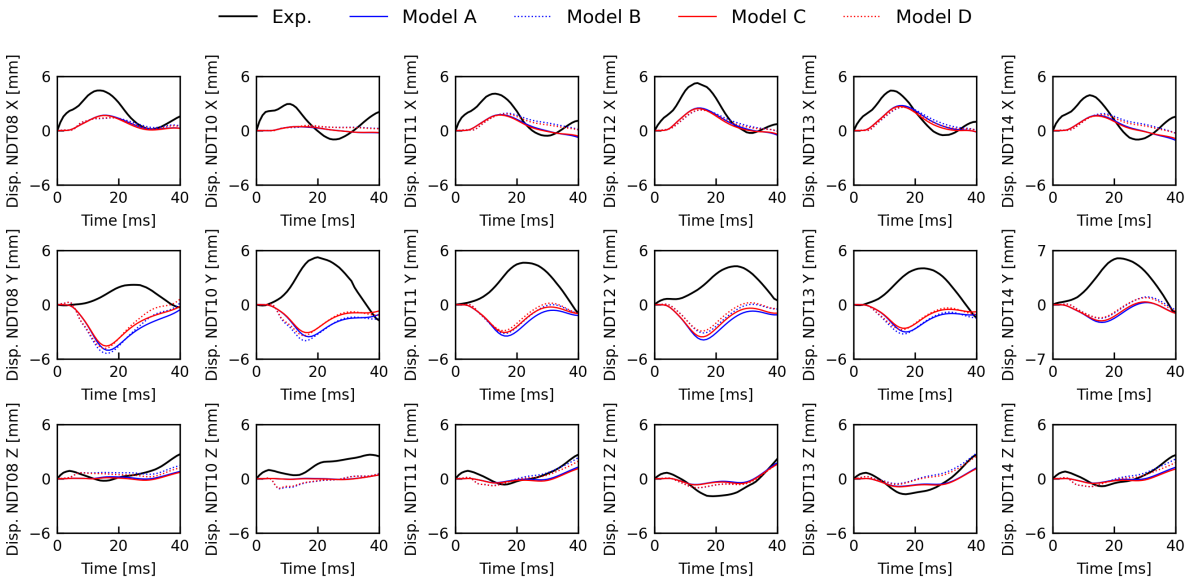

Figure A4. Comparisons of the histories of displacements in NDTs belonging to C2 for C380-T2 between the PMHS test data [24] and the simulation results.

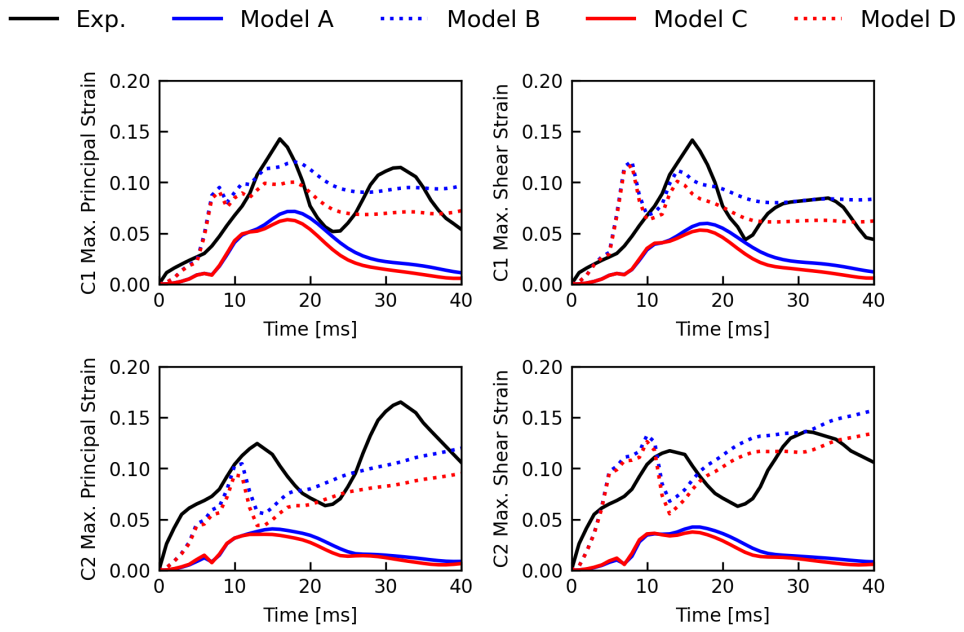

Figure A5. Comparisons of the histories of strain in C1 and C2 for C288-T3 between the PMHS test data [24, 27] and the simulation results.

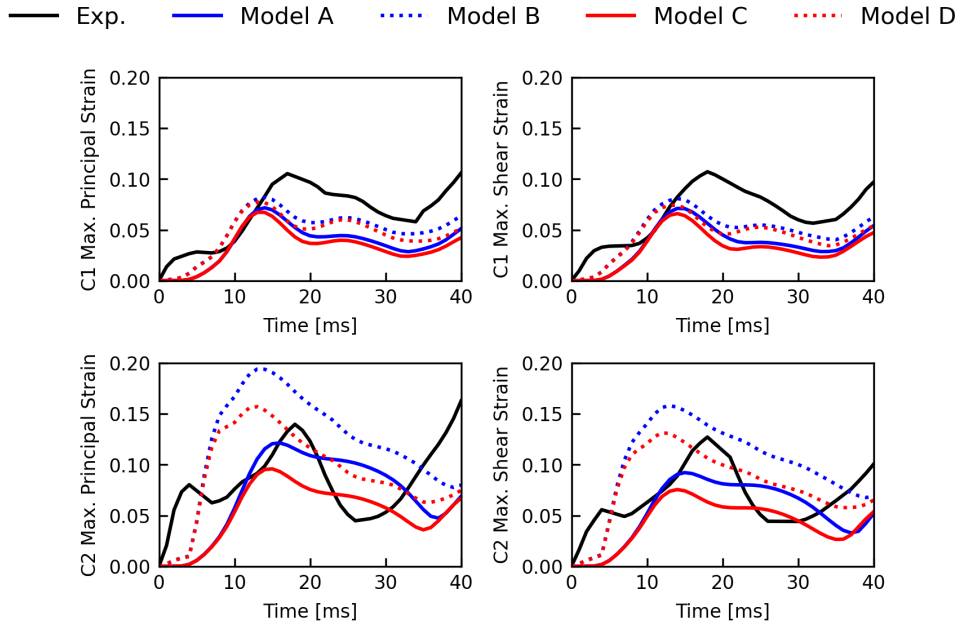

Figure A6. Comparisons of the histories of strain in C1 and C2 for C380-T1 between the PMHS test data [24, 27] and the simulation results.